

Received: 2020.03.16

Accepted: 2020.05.14

Available online: 2020.08.17

Published: 2020.10.02

Circular RNA circ_C16orf62 Suppresses Cell Growth in Gastric Cancer by miR-421/Tubulin beta-2A Chain (TUBB2A) Axis

Authors' Contribution:
Study Design A
Data Collection B
Statistical Analysis C
Data Interpretation D
Manuscript Preparation E
Literature Search F
Funds Collection G

ABCDE 1 **Yanfeng Jin**
BCDEF 1 **Shanshan Zhang**
BCDE 2 **Li Liu**

1 Department of Gastroenterology, Yantai Yuhuangding Hospital, Yantai, Shandong, P.R. China
2 Department of Oncology, The Second Hospital of Weifang, Weifang, Shandong, P.R. China

Corresponding Author: Li Liu, e-mail: waqhtn@163.com
Source of support: Departmental sources

Background: Gastric cancer (GC) is the third leading cause of cancer-associated mortality in the world. Expression of circular RNA circ_C16orf62 is reported to be low in GC. The role and mechanism of circ_C16orf62 remain unclear.





Material/Methods: Expression levels of circ_C16orf62 and tubulin beta-2A chain (TUBB2A) in GC tissues and cells, and microRNA-421 (miR-421) level in GC cells were detected by real-time quantitative polymerase chain reaction (RT-qPCR). The predominant cytoplasmic localization of circ_C16orf62 was identified by subcellular fractionation. The protein level of TUBB2A was detected by western blot assay. Cell proliferative ability, migration, and invasion were measured by 3-(4, 5-dimethyl-2-thiazolyl)-2, 5-diphenyl-2-H-tetrazolium bromide (MTT), colony formation, and several transwell assays. The binding relationship between miR-421 and circ_C16orf62 or TUBB2A was predicted by starBase3.0 or Targetscan, and then verified by the dual-luciferase reporter assay. The biological role of circ_C16orf62 was examined by xenograft tumor model *in vivo*.

Results: Circ_C16orf62 and TUBB2A were downregulated in GC tissues and cells. Circ_C16orf62 was predominantly located in the cytoplasm of GC cells, and repressed proliferation, migration, and invasion of GC cells. Mechanistically, circ_C16orf62 worked as the miR-421 sponge to upregulate TUBB2A in GC, thereby hindering GC growth. Circ_C16orf62 repressed GC tumor growth *in vivo*.

Conclusions: These findings demonstrate that circ_C16orf62 impeded proliferation, migration, and invasion *in vitro* and retarded tumor growth *in vivo* by the miR-421/TUBB2A axis in GC, providing a potential therapeutic strategy for patients with GC.

MeSH Keywords: **Cell Growth Processes • Prognosis • Stomach Neoplasms**

Full-text PDF: <https://www.medscimonit.com/abstract/index/idArt/924343>

 3021  —  9  31



Background

Gastric cancer (GC), an intractable malignancy, is the third most common cause of cancer-related death worldwide [1]. In 2019, there were approximately 27,510 new cases of and 11,140 deaths from GC in the United States [2]. Despite the substantial progress in diagnosis and therapeutic methods, the overall prognosis for patients with GC is still unsatisfactory [3]. Therefore, to develop more effective therapeutic targets, it is imperative to explore the underlying molecular mechanisms of GC.

Recently, circular RNAs (circRNAs), a novel class of non-coding transcripts with covalently closed-loop, have been confirmed to be extensively expressed in a variety of mammalian cells [4,5]. Accumulating evidence indicates that abnormal expression of circRNAs plays a role in the formation and development of multiple cancers [6–9]. For example, overexpression of circ-Cdr1as hindered bladder cancer by inhibiting proliferation, migration, and invasion through binding to miR-135a [10]. Moreover, circ-BANP was shown to be involved in modulating lung cancer growth and metastasis by sponging 503 from LARP1 [11]. A recent publication showed that circular RNAs circ_C16orf62 (hsa_circ_0005699), located on chromosome 16, was reported to be downregulated in GC [12]. However, the role and functional mechanism of circ_C16orf62 have not been determined.

Over the last decade, microRNAs (miRNAs), an endogenous non-coding RNA with 19 to 25 nucleotides, have been shown to negatively regulate gene expression by binding to the 3'-untranslated region (3'UTR) of target mRNAs [13,14]. A substantial body of research shows that miRNAs, as oncogenes or suppressors, may play a role in development and progression of GC. For instance, Li et al. reported that the abundance of miR-543 contributed to GC cell proliferation and cell cycle progression through improving SIRT1 expression [15]. Sun et al. confirmed that miR-338-3p worked as a tumor suppressor to impede migration and induce apoptosis in GC by interacting with PTP1B [16]. MicroRNA-421 (miR-421), a new diagnostic biomarker [17], acted as a carcinogenic factor in GC to accelerate proliferation and metastasis by blocking claudin-11 expression [18]. Nevertheless, the precise mechanism of miR-421 in GC requires further exploration.

Tubulin beta-2A chain (TUBB2A), a member of tubulin subunits, accounts for 30% of β -tubulin in the human brain [19]. Furthermore, previous literature shows that grifola frondosa glycoprotein (GFG3a) can constrain cell cycle and boost apoptosis of GC cells by downregulating TUBB2A expression [20], suggesting that TUBB2A might act as a tumor suppressor in GC progression.

In this paper, we show that circ_C16orf62 and TUBB2A were downregulated in GC tissues and cells. Moreover, our data confirm the cytoplasmic localization of circ_C16orf62. Therefore, the function and molecular mechanisms of circ_C16orf62 in proliferation, migration and invasion of GC cells were further investigated.

Material and Methods

Clinical samples and cell culture

The study was approved by the ethical committee of Yantai Yuhuangding Hospital and written informed consent was collected from each patient. Human GC tissues (n=32) and matched normal tissues were provided by the patients from Yantai Yuhuangding Hospital.

GC cell lines MKN-74, HGC-27 and AGS were collected from the Japanese Cancer Resources Bank (JCRB, Tokyo, Japan) and Cell Bank of the Chinese Academy of Sciences (Shanghai, China). A human normal gastric epithelial cell line (GES-1) was obtained from the Beijing Institute of Cancer Research (Beijing, China). Cells were maintained at 37°C in a 5% CO₂ in Roswell Park Memorial Institute medium 1640 (RPMI-1640; Gibco, Grand Island, New York, United States) with 10% fetal bovine serum (FBS; Gibco), 10% penicillin-streptomycin (100 U/mL, 100 mg/mL, Gibco).

Real-time quantitative polymerase chain reaction (RT-qPCR)

GC tissues and cells were lysed based on the supplier's direction for TRIzol reagent (Gibco). Quantification of extracted RNA was analyzed by using NanoDrop. The first-strand complementary DNA (cDNA) of circ_C16orf62, miR-421 and TUBB2A were synthesized with PrimeScriptRT Reagent Kit (Takara, Dalian, China). RT-qPCR was conducted on ABI 7500 real-time PCR system (Applied Biosystems, Foster City, CA, USA) with SYBR Green PCR kit (Takara). Gene relative expression was calculated following the 2^{- $\Delta\Delta Ct$} method [21], normalizing with glyceraldehyde-3-phosphate dehydrogenase (GAPDH) or U6. The primers sequences were displayed as follows:
circ_C16orf62: 5'-TCCCCTGTACGAAATCATTCCA-3' (sense),
5'-ATTGAGACGTGTGAAGATGCCC-3' (antisense);
C16orf62: 5'-TCAATGCGTAAATCGGTTGGC-3' (sense),
5'-GCTGCTGCTTTTGTAGTGTGG-3' (antisense);
miR-421: 5'-GATTGCACGTTTTTCAGGTG-3' (sense),
5'-GCAGCACATCATTATTACA-3' (antisense);
TUBB2A: 5'-TCCGAGTACCAGCAGTACCA-3' (sense),
5'-AAGAAAGTTGGTAAGCCTCG-3' (antisense);
U6: 5'-GCTCGCTCGGCAGCACA-3' (sense),
5'-GAGGTATTGCACAGAGGA-3' (antisense);

GAPDH: 5'-GTCAACGGATTTGGTCTGTATT-3' (sense),
5'-AGTCTTCTGGGTGGCAGTGAT-3' (antisense).

Western blot assay

Western blot assay was implemented to examine the protein level of TUBB2A in AGS and HGC-27 cells. Generally, GC cell lysates were harvested with radioimmunoprecipitation buffer (RIPA, Beyotime, Shanghai, China) including protease inhibitor (Beyotime), and quantified by bicinchoninic acid (BCA, Beyotime). Extracted proteins were treated with sodium dodecyl sulfate-polyacrylamide gel electrophoresis (SDS-PAGE), and transferred onto nitrocellulose membranes (Millipore Corp, Bedford, MA, USA), followed by blockage with 5% skim milk for 2 h. After incubating with primary antibodies against TUBB2A (1: 1000, ab170931, Abcam, Cambridge, MA, USA) and β -actin (1: 1000, ab52614, Abcam) at 4°C all night, membranes were incubated with the horseradish peroxidase (HRP)-conjugated secondary antibody for 2 h. At last, bands were detected by enhanced chemiluminescence reagent (ECL, Pierce Biotechnology, Rockford, Illinois, United States).

RNase R treatment

Total RNA was incubated at 37°C for 15 min, with or without RNase R (3 U/mg, Epicentre, Shanghai, China). Subsequently, treated RNA was purified by using phenol-chloroform (Sigma, St. Louis, Mo, USA). Whereafter, RT-qPCR assay was used to examine levels of circ_C16orf62 and C16orf62 mRNA.

Subcellular fractionation assay

To isolate cytoplasmic and nuclear RNA in GC cells, AGS and HGC-27 cells were incubated and centrifuged in cytoplasm lysis buffer, followed by collection of the cytoplasmic supernatant. The remainder was incubated and centrifuged in nucleus lysis buffer. All RNAs were extracted from cytoplasmic and nuclear by using TRIzol reagent (Gibco). Finally, RT-qPCR was applied to measure the levels of circ_C16orf62, GAPDH (cytoplasm control) and U6 (nucleus control) in cytoplasmic and nuclear.

Cell transfection

The overexpression plasmid of circ_C16orf62 or TUBB2A was constructed by inserting sequences of circ_C16orf62 or TUBB2A into the pcDNA 3.1 vector (pcDNA, Invitrogen, Carlsbad, CA, USA), named as pcDNA-circ_C16orf62 (circ_C16orf62) or pcDNA-TUBB2A (TUBB2A), and pcDNA empty plasmid (NC or pcDNA, as a negative control). Circ_C16orf62 small interference RNA (si-circ_C16orf62), TUBB2A small interference RNA (si-TUBB2A #1, #2, #3) and their negative control (si-NC), miR-421 mimic (miR-421) and its negative control (miR-NC), miR-421 inhibitor (anti-miR-421) and its negative control (anti-miR-NC) were

purchased from GenePharma (Shanghai, China). Thereafter, AGS and HGC-27 cells (4×10^5 cells/well) were transfected with the plasmids and oligonucleotides as per the user's guidebook for the Lipofectamine 3000 reagent (Invitrogen), respectively. After 48-h incubation, transfected cells were harvested and used in the following assays.

Cell viability assay

3-(4, 5-dimethyl-2-thiazolyl)-2, 5-diphenyl-2-H-tetrazolium bromide (MTT, 5 mg/mL) obtained from Sigma was implemented to test the proliferation ability of GC cells. Transfected AGS and HGC-27 cells were incubated in a 96-well plate at a density of 2×10^3 cells/well, followed by culturing for 0, 1, 2, or 3 days. Subsequently, MTT (20 μ L, Sigma) was added into each well for another 4 h, after which the supernatant was discarded. Finally, 150 μ L dimethyl sulfoxide (DMSO, Sigma) was applied to dissolve the formed formazan crystals, and the absorbance at a wavelength of 490 nm was measured under a microplate reader (Tecan, Switzerland).

Colony formation assay

In short, transfected AGS and HGC-27 cells (4×10^2 cells) were seeded into six-well plates and cultured at 37°C for 2 weeks. After washing with phosphate buffered saline (PBS, Invitrogen), the number of colonies per well were fixed with methanol and stained with 0.1% crystal violet solution, and then imaged and counted.

Transwell assay

Transwell chambers (24-well, Chemicon, Temecula, California, United States) were applied for detection the migration and invasion abilities of GC cells according to the operation manual. Remarkably, the upper chambers of transwell were precoated with Matrigel (BD Biosciences, San Jose, California, United States) for invasion assay. Briefly, transfected GC cells in serum-free medium were introduced into the upper chambers, and the medium containing 10% FBS (Gibco, as chemoattractant) was added into the lower chambers. At 24 h post-incubation, the cells on the upper surface were removed with a cotton swab, while the cells on the lower surface were stained with 0.1% crystal violet, followed by photographing with a microscope (Tecan).

Dual-luciferase reporter assay

The sequences of circ_C16orf62 and TUBB2A 3' untranslated regions (utr) containing wild-type (wt) or mutant-type (mut) miR-421 binding sites were amplified by PCR. Then, these sequences were inserted into pGL3 luciferase reporter vectors (Promega, Fitchburg, WI, USA), termed as circ_C16orf62-wt,

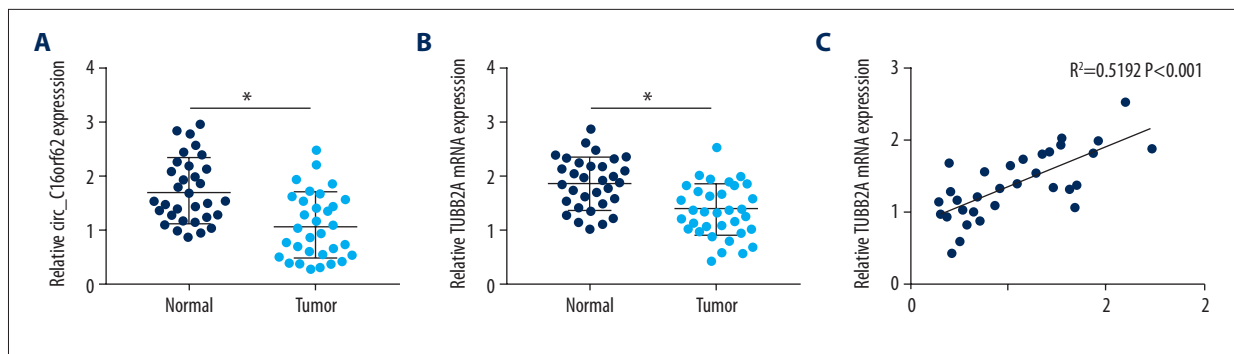


Figure 1. Circ_C16orf62 and TUBB2A were decreased in GC tissues. (A, B) RT-qPCR assay was applied to measure expression of circ_C16orf62 and TUBB2A in 32 pairs of GC tumor tissues and adjacent normal tissues. (C) The expression association between circ_C16orf62 and TUBB2A in GC tumor tissues was analyzed by Pearson correlation analysis. * $P < 0.05$.

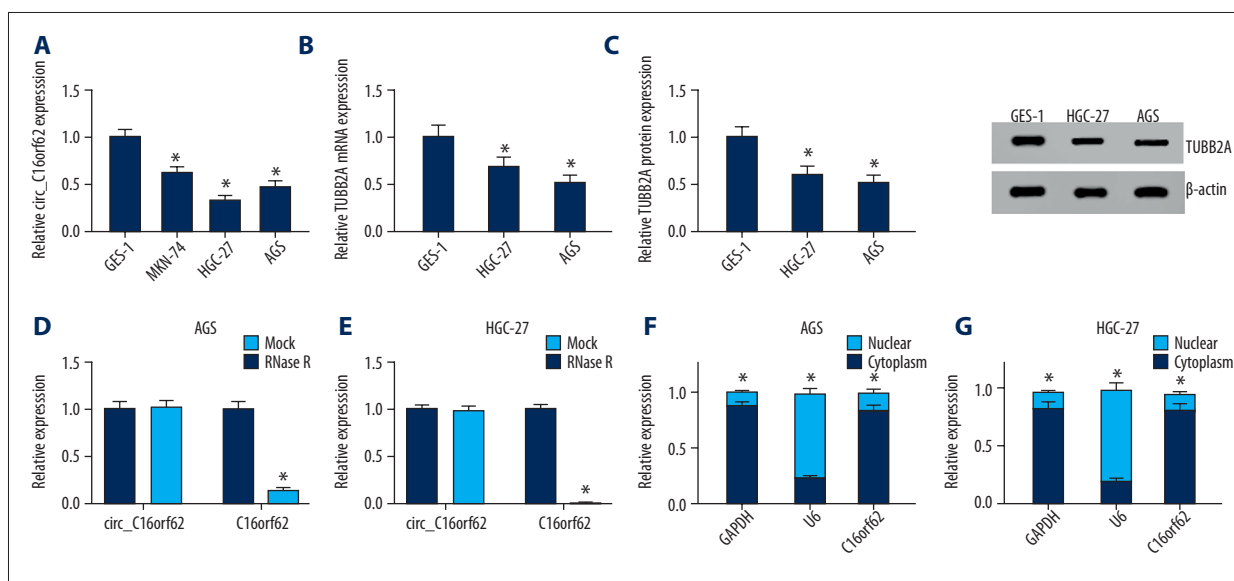


Figure 2. Circ_C16orf62 was expressed at low level in GC cells. (A) Expression of circ_C16orf62 in human normal gastric epithelial cell line (GES-1) and GC cell lines (MKN-74, HGC-27 and AGS) detected by RT-qPCR assay. (B, C) TUBB2A levels in human normal gastric epithelial cell line (GES-1) and GC cell lines (HGC-27 and AGS) were measured by RT-qPCR and western blot assays. (D, E) Relative levels of circ_C16orf62 and C16orf62 mRNA were tested in HGC-27 and AGS cells treated with or without RNase R. (F, G) The cellular localization of circ_C16orf62 in AGS and HGC-27 cells was analyzed by subcellular fractionation assay. * $P < 0.05$.

circ_C16orf62-mut, TUBB2A-wt and TUBB2A-mut reporter plasmids. With the help of Lipofectamine 3000 (Invitrogen), AGS and HGC-27 cells were transfected with these constructed reporter plasmids and miR-421 mimic or miR-NC, respectively. Dual-luciferase reporter assay kit (Promega) was conducted to analyze the luciferase activities.

Tumor xenograft assay

Lentiviral vector (Lenti-PCDH-circ_C16orf62) for stable circ_C16orf62 overexpression, and the scramble control vector (PCDH-NC) were provided by Genechem (Shanghai, China). Male BALB/C nude mice (n=12) that were 4 weeks old were

obtained from the Hubei Research Center of Laboratory Animal (Wuhan, China). This study was approved by the Institutional Committee for Animal Research of the Yantai Yuhuangding Hospital. AGS cells (2×10^6) transduced with PCDH-circ_C16orf62 or PCDH-NC were subcutaneously injected into the left flank of the nude mice (n=6 per group). At 10 days after injection, tumor volume was measured every 4 days. Thirty-four days later, tumors were excised and weighed.

Statistical analysis

Data were analyzed by using GraphPad Prism7 software, and presented as mean \pm standard deviation (SD). Data differences

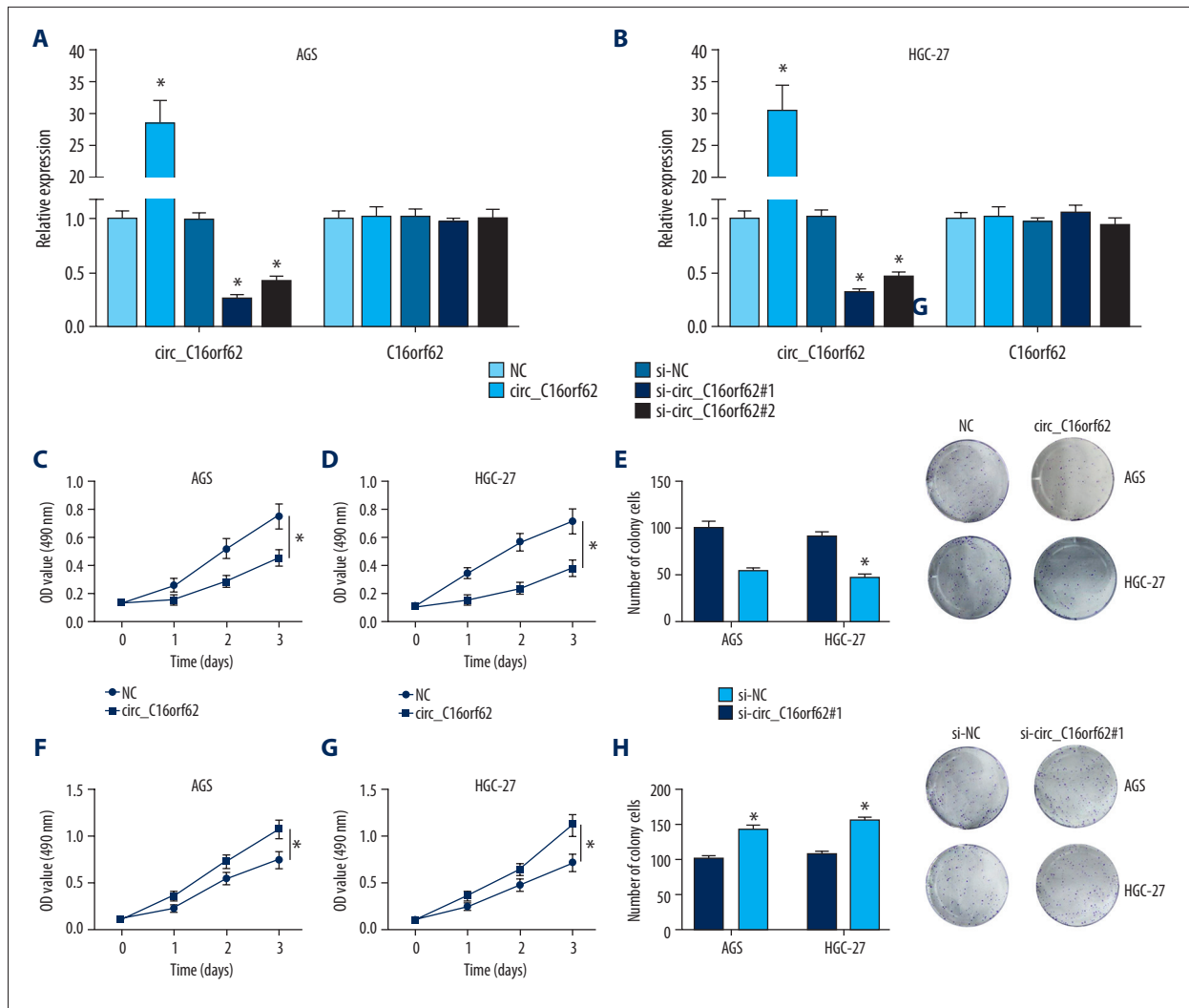


Figure 3. Circ_C16orf62 suppressed proliferation of GC cells *in vitro*. (A, B) Circ_C16orf62 expression level was assessed in AGS and HGC-27 transfected with NC, circ_C16orf62, si-NC, si-circ_C16orf62#1 and si-circ_C16orf62#2. (C–E) MTT and colony formation assays were carried out to measure the proliferative ability of cells transfected with circ_C16orf62 and empty vector. (F–H) Proliferative ability was examined in si-NC or si-circ_C16orf62#1-transfected AGS and HGC-27 cells. * $P < 0.05$.

between two or multiple groups were assessed with student's *t*-test or one-way analysis of variance (ANOVA). Statistical significance was considered as $P < 0.05$.

Results

Circ_C16orf62 and TUBB2A were downregulated in GC tissues

First, to explore the function of circ_C16orf62 and TUBB2A in GC, their expression levels were examined in GC tumor tissues. Compared with 32 adjacent normal tissues, circ_C16orf62 and TUBB2A were expressed at a low level in 32 GC tumor tissues (Figure 1A, 1B). Furthermore, circ_C16orf62 levels were

positively related to the expression level of TUBB2A in GC tumor tissues (Figure 1C). Together, these data indicate that circ_C16orf62 and TUBB2A are involved in GC progression.

Circ_C16orf62 and TUBB2A were decreased in GC cells

Given that circ_C16orf62 and TUBB2A were downregulated in GC tumor tissues, we further investigated their expression in GC cells. As presented in Figure 2A, the expression levels of circ_C16orf62 were markedly lower in GC cell lines (MKN-74, HGC-27 and AGS) relative to the human normal gastric epithelial cell line GES-1. Because that was true, in particular, in HGC-27 and AGS cells, the TUBB2A level was examined in those two cell lines. Data suggested that TUBB2A expression was lower in HGC-27 and AGS cells than in GES-1

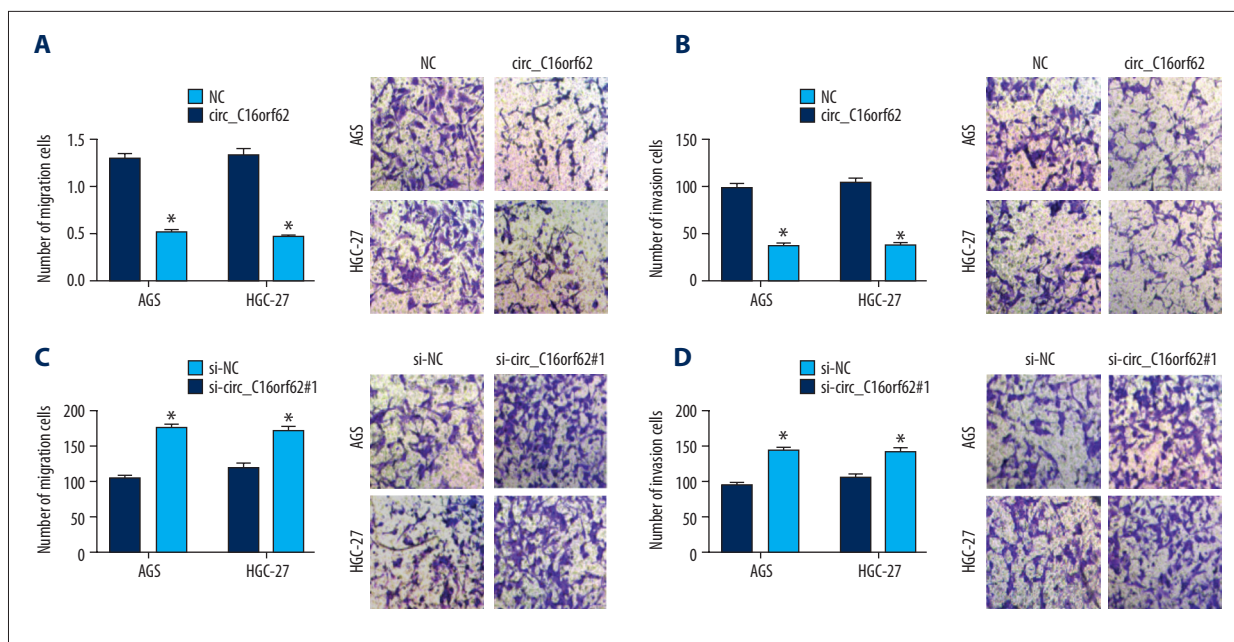


Figure 4. Circ_C16orf62 repressed migration and invasion of GC cells *in vitro*. (A, B) Transwell migration assay was applied to assess the capacity of migration and in NC or circ_C16orf62-transfected H460 and A549 cells. (C, D) Invasion ability was measured by transwell invasion assay in si-NC or si-circ_C16orf62#1-transfected AGS and HGC-27 cell. * $P < 0.05$.

cells (Figure 2B, 2C). These results further confirmed that circ_C16orf62 and TUBB2A might play a role in progression of GC. To further explore the stability and localization of circ_C16orf62 in GC cells, we used a highly processive 3' to 5' exonuclease (RNase R enzyme) that does not act on linear rather than circular RNA. As shown in Figure 2D and 2E, RNase R treatment effectively downregulated the C16orf62 mRNA level but had no effect on circ_C16orf62, demonstrating that circ_C16orf62 was indeed a circular RNA. Moreover, subcellular localization of circ_C16orf62 was further investigated through nuclear and cytoplasmic separation assays. As a result, we found that circ_C16orf62 was predominantly localized in cytoplasm of AGS and HGC-27 cells (Figure 2F, 2G). In short, circ_C16orf62 possessed a loop structure and was mainly localized in the cytoplasm.

Circ_C16orf62 impeded proliferative ability of GC cells *in vitro*

To further verify the role of circ_C16orf62 in GC cells, we over-expressed or knocked down circ_C16orf62 expression in AGS and HGC-27 cells. Subsequently, their transfection efficiency was measured, as shown in Figure 3A and 3B. Moreover, in MTT and colony formation assays, we observed that circ_C16orf62 overexpression hindered the proliferative ability of AGS and HGC-27 cells (Figure 3C–3E). On the contrary, circ_C16orf62 deletion led to remarkable enhancement in the proliferative ability of these two cell lines (Figure 3F–3H). Collectively, circ_C16orf62 curbed the proliferative ability of GC cells.

Circ_C16orf62 inhibited migration and invasion of GC cells *in vitro*

Next, we explored the effect of circ_C16orf62 on migration and invasion in GC cells. As shown in Figure 4A and 4B, cell migration and invasion were strikingly blocked after upregulation of circ_C16orf62. However, the opposite results were seen in two cell lines transfected with si-circ_C16orf62#1, as circ_C16orf62 deficiency obviously accelerated migration and invasion in AGS and HGC-27 cells (Figure 4C, 4D). Overall, circ_C16orf62 hampered migration and invasion of GC cells.

TUBB2A constrained proliferation, migration, and invasion of GC cells *in vitro*

Considering the low expression of TUBB2A in GC cells, an over-expressing plasmid of TUBB2A was constructed. Data showed that the TUBB2A level was notably upregulated in AGS and HGC-27 cells transfected with TUBB2A versus cells with pcDNA (Figure 5A, 5B). Functionally, the proliferative ability of AGS and HGC-27 cells was drastically suppressed after introduction of TUBB2A (Figure 5C–5E). Meanwhile, decreased cell migration and invasion were demonstrated in response to up-regulation of TUBB2A in AGS and HGC-27 cells (Figure 5F, 5G). In a word, TUBB2A hindered proliferation, migration, and invasion in GC cells.

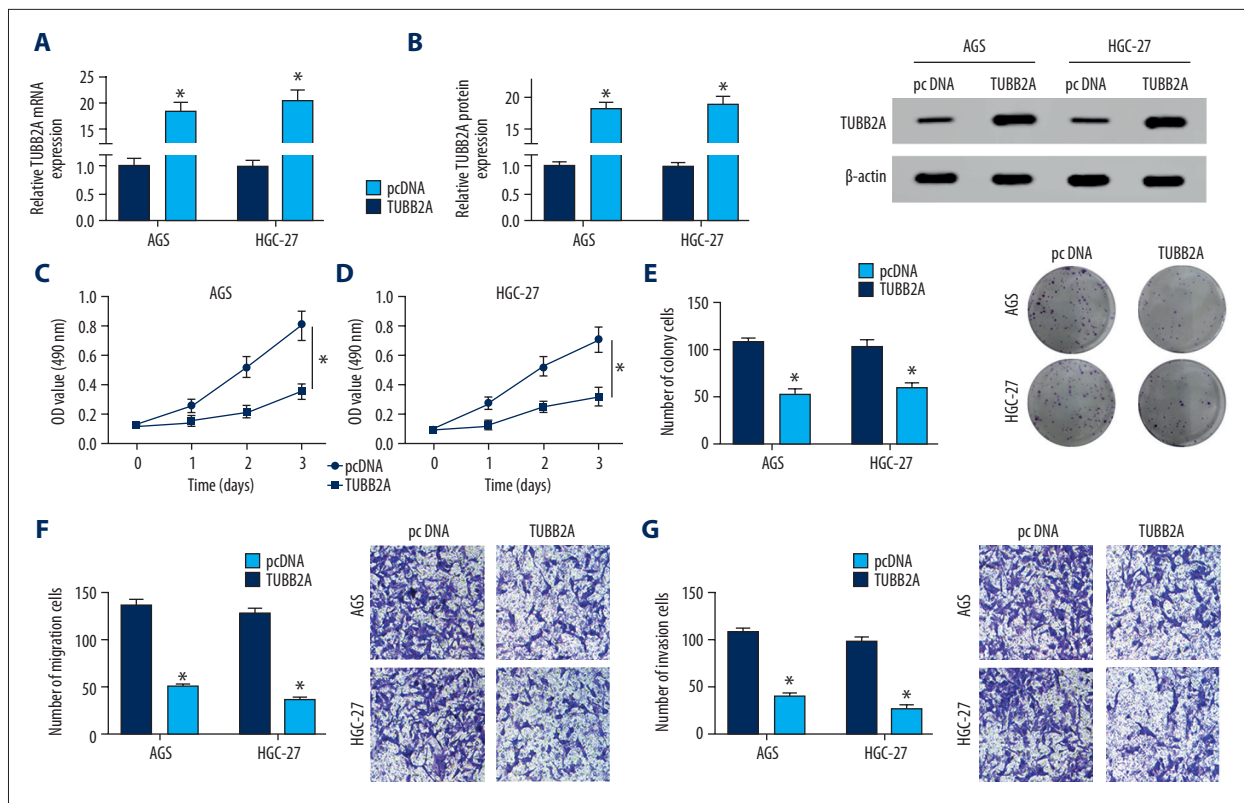


Figure 5. TUBB2A inhibited proliferation, migration and invasion of GC cells *in vitro*. (A, B) TUBB2A level was detected by RT-qPCR and western blot assays in AGS and HGC-27 cells transfected with pcDNA or TUBB2A. (C–E) MTT and colony formation assays were applied to assess the proliferative ability in pcDNA or TUBB2A-transfected AGS and HGC-27 cells. (F, G) Transwell assay was applied to assess the capacities of migration and invasion in pcDNA or TUBB2A-transfected AGS and HGC-27 cells. * $P < 0.05$.

Circ_C16orf62 and TUBB2A directly bound with miR-421 in GC cells

As is widely accepted, circRNA could impact mRNA expression by interacting with miRNA [22]. To probe the mechanism of circ_C16orf62 in GC cells, bioinformatics software StarBase3.0 was applied. As exhibited in Figure 6A, miR-421 was found to contain some binding sites with circ_C16orf62. A dual-luciferase reporter assay then was used to further confirm the predictive result. Data showed that the overexpression of miR-421 reduced the luciferase activity of circ_C16orf62-wt reporter, while it had no effect on the luciferase activity of circ_C16orf62-mut in AGS and HGC-27 cells (Figure 6B, 6C). Simultaneously, RT-qPCR assay proved that the circ_C16orf62 level was negatively associated with miR-421 level in GC cells (Figure 6D, 6E). Interestingly, through bioinformatics software Targetscan, we found that miR-421 also had some complementary base pairing with TUBB2A (Figure 6F), as demonstrated by dual-luciferase reporter assay (Figure 6G, 6H). Moreover, transfection efficiency of miR-421 mimics or anti-miR-421 was detected by RT-qPCR assay in GC cells (Figure 6I). Synchronously, there existed inverse correlation between miR-421 and TUBB2A in

AGS cells (Figure 6J, 6L) and HGC-27 cells (Figures 6K, 6M). All of these results suggested that circ_C16orf62 might regulate TUBB2A expression by targeting miR-421 in GC cells.

Verification of Circ_C16orf62/miR-421/TUBB2A regulatory axis in GC cells

Next, to further confirm whether circ_C16orf62 could exert its role in a miRNA-mRNA-dependent manner, rescue assays were conducted in GC cells. As illustrated in Figure 7A, 7B, circ_C16orf62 overexpression facilitated expression of TUBB2A in AGS and HGC-27 cells, while miR-421 upregulation or TUBB2A knockdown apparently abolished the circ_C16orf62-mediated promoting effect on TUBB2A level. This assay validated that circ_C16orf62 could act as a sponge of miR-421 to affect TUBB2A expression in GC cells.

Circ_C16orf62 suppressed GC progression by miR-421/TUBB2A axis

Furthermore, to prove the function of circ_C16orf62/miR-421/TUBB2A axis in regulating GC tumor progress, functional assays

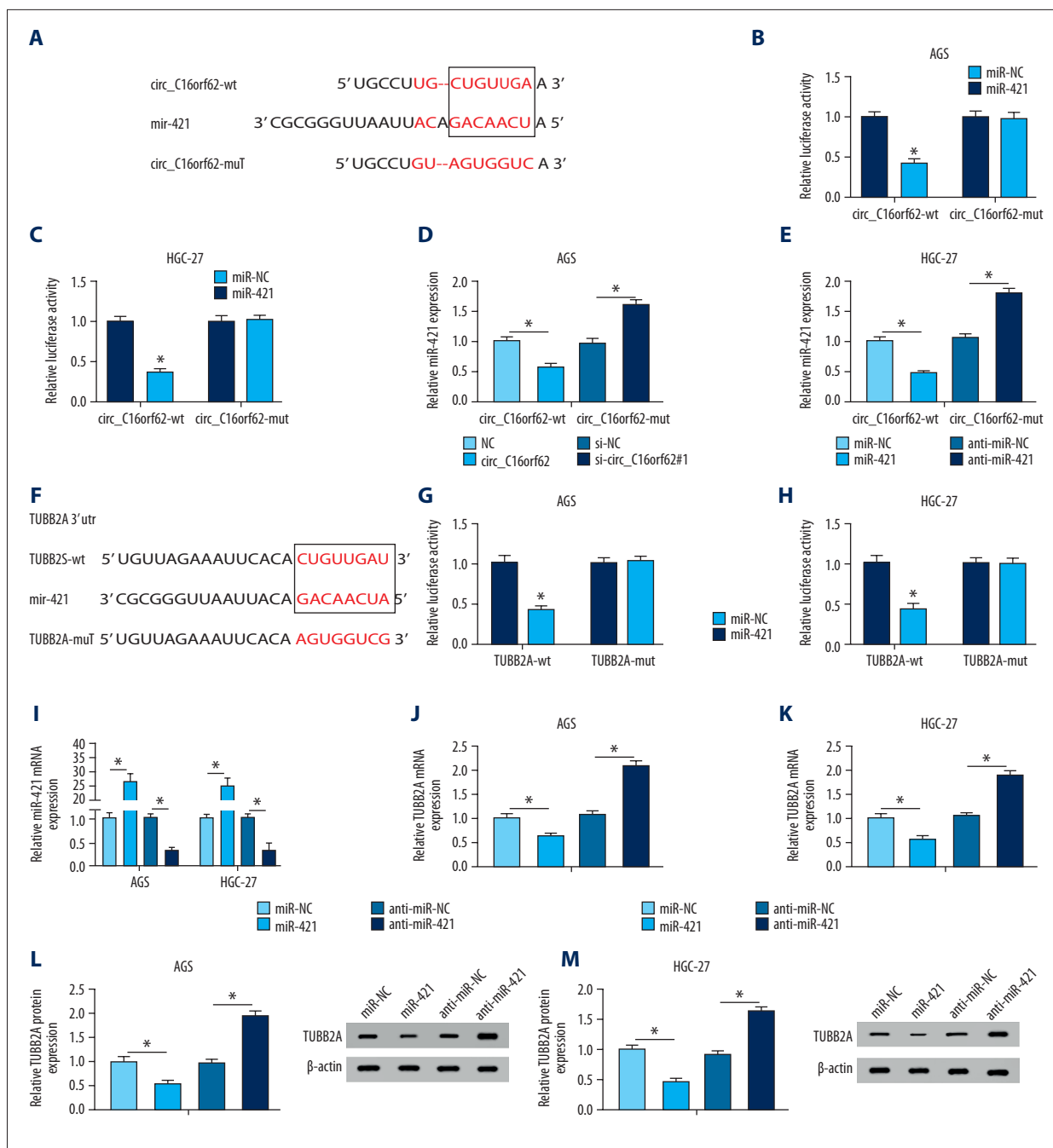


Figure 6. Circ_C16orf62 and TUBB2A bound to miR-421 in GC cells. (A) The binding sites between circ_C16orf62 and miR-421 were predicted by bioinformatics software StarBase3.0. (B, C) The binding relationship between circ_C16orf62 and miR-421 were testified by dual-luciferase reporter assay. (D, E) MiR-421 level was measured in AGS and HGC-27 transfected with NC, circ_C16orf62, si-NC and si-circ_C16orf62#1. (F) The binding sequences between TUBB2A and miR-421 were predicted by bioinformatics software Targetscan. (G, H) Relative luciferase activity was determined by dual-luciferase reporter assays in AGS and HGC-27 cells co-transfected with reporter plasmid (TUBB2A-wt/TUBB2A-mut) and miR-421 or miR-NC. (I) Transfection efficiency of miR-421 mimic or anti-miR-421 was detected by RT-qPCR assay. (J, K) The effects of miR-421 overexpression or miR-421 knockdown on TUBB2A mRNA level were tested by RT-qPCR assay. (L, M) TUBB2A protein level was examined in miR-421 or anti-miR-421-transfected AGS and HGC-27 cells. * $P < 0.05$.

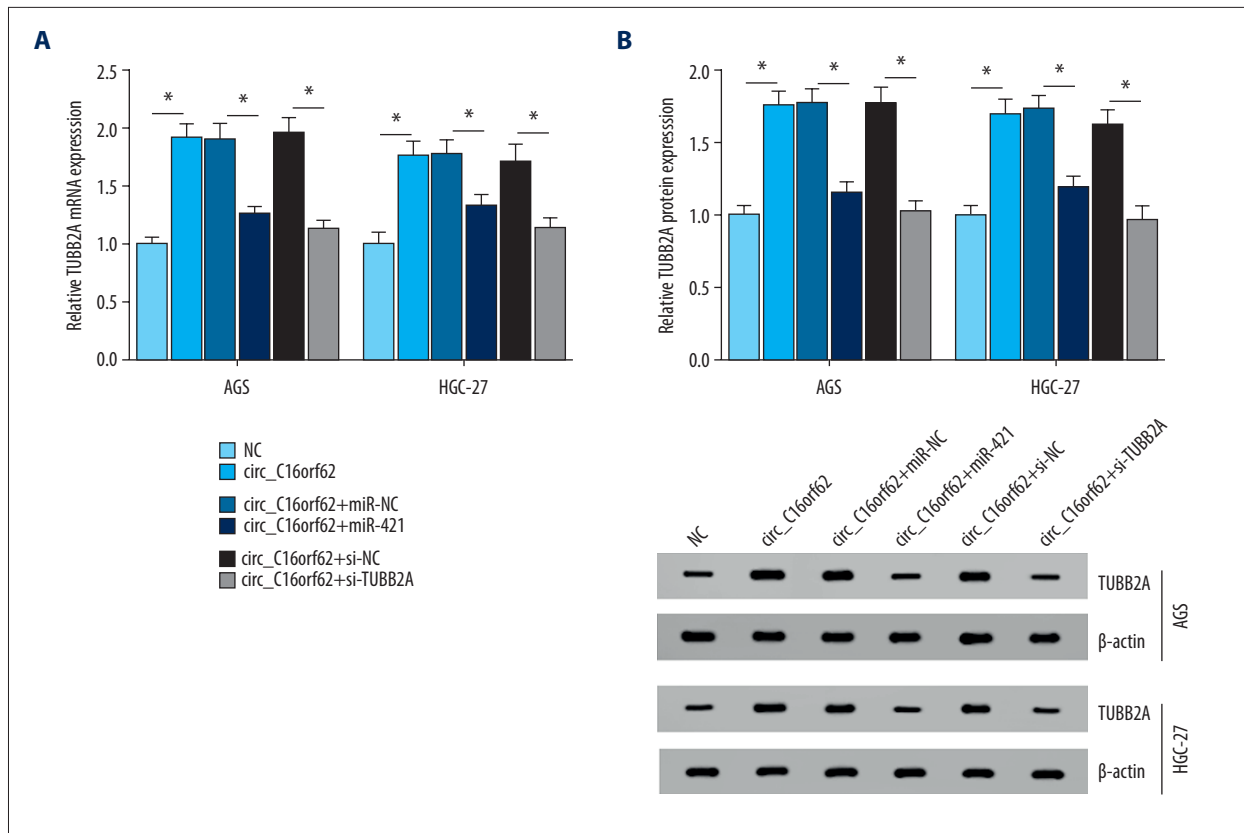


Figure 7. Circ_C16orf62 elevated TUBB2A expression by sponging miR-421 in GC cells. **(A, B)** TUBB2A level was detected in AGS and HGC-27 cells transfected with NC, circ_C16orf62, circ_C16orf62+ miR-NC, circ_C16orf62+ miR-421, circ_C16orf62+ si-NC and circ_C16orf62+si-TUBB2A. * $P < 0.05$.

were performed in GC cells. First, MTT and colony formation assays revealed that suppression of proliferative ability due to circ_C16orf62 overexpression was overturned through miR-421 mimic or si-TUBB2A in AGS and HGC-27 cells (Figure 8A–8C). Apart from that, miR-421 overexpression or TUBB2A silencing partly abrogated the inhibitory effect of circ_C16orf62 on migration and invasion in AGS and HGC-27 cells (Figure 8D, 8E). Taken together, we concluded that circ_C16orf62 could repress GC progression by modulating miR-421/TUBB2A axis.

Circ_C16orf62 inhibited GC cell growth *in vivo*

In addition, a mice xenograft model of GC was constructed to probe the effect of circ_C16orf62 on tumor growth. As shown in Figure 9A, 9B, tumor volume and weight were reduced in the presence of circ_C16orf62 upregulation, testifying that circ_C16orf62 could retard tumor growth *in vivo*. In addition, RT-qPCR and western blot assay verified that expression of circ_C16orf62 and TUBB2A was increased in tumor tissues derived from PCDH-circ_C16orf62-transfected AGS cells (Figure 9C–9E), while the miR-421 level was reduced in the tumor tissues (Figure 9F). All of these might suggest that

circ_C16orf62 suppressed GC tumor growth, possibly by regulating miR-421/TUBB2A axis *in vivo*.

Discussion

Increasing evidence indicates that circRNAs are implicated in initiation and progression of diverse cancers [23,24]. CircRNA_0001429 acted as an oncogene in bladder cancer to facilitate propagation and metastasis, and to repress apoptosis by sponging miR-205 to increase VEGFA expression [25]. CircRNA_HIAT1 served as a competing endogenous RNA (ceRNA) in hepatocellular carcinoma to hamper cell growth by modulating the miR-3171/PTEN axis [26]. Notably, it was previously reported that circ_C16orf62 expression was decreased in GC [12]. Nevertheless, whether circ_C16orf62 is involved in progression of GC and its molecular mechanism is still unknown. In this paper, circ_C16orf62 expression was low in GC tissues and cells, consistent with previous reports [12]. We further explored the biological function of circ_C16orf62 in GC cells. Functional analysis revealed that circ_C16orf62 could exert an inhibitory effect on GC growth *in vitro* and *in vivo*.

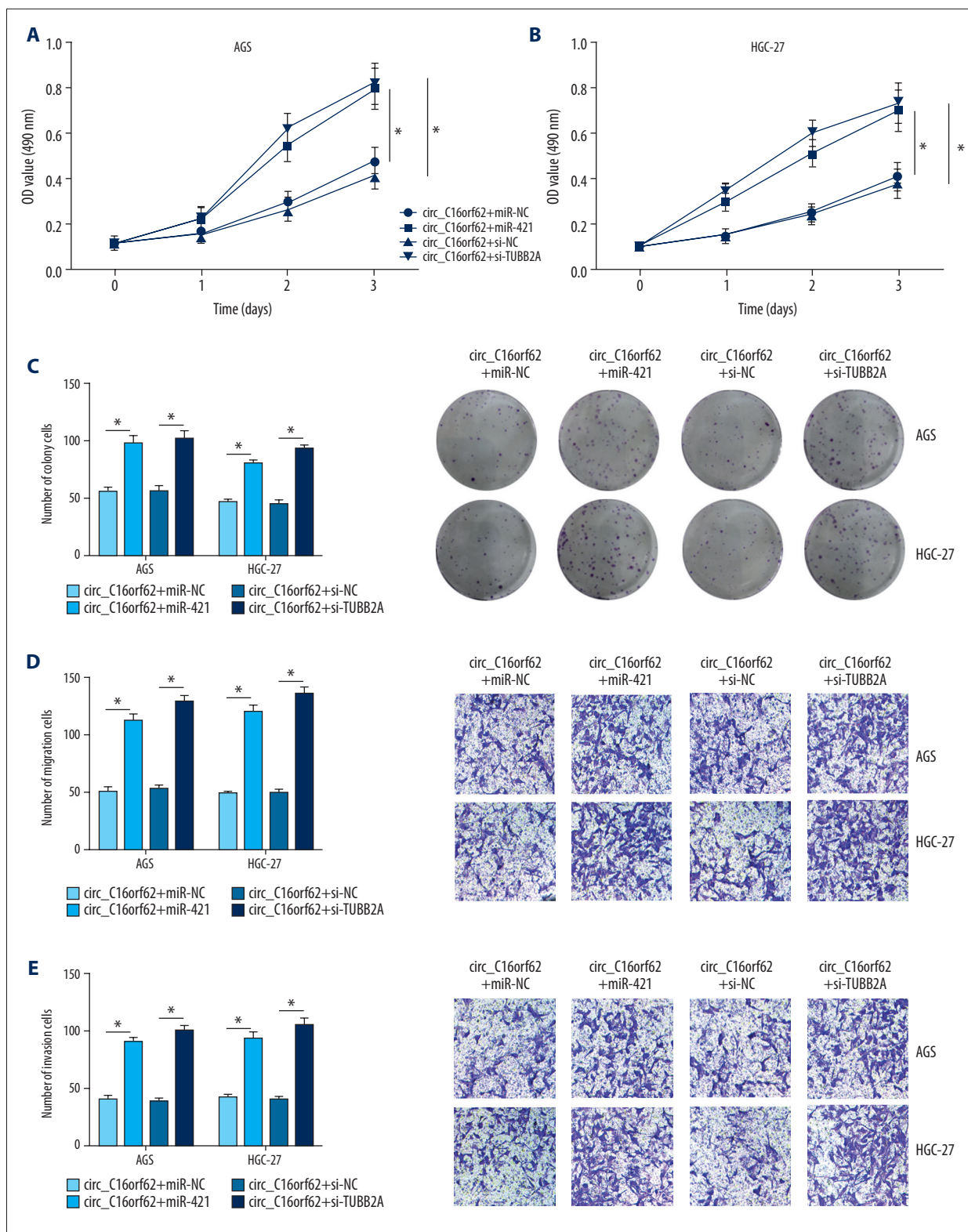


Figure 8. Circ_C16orf62 hindered tumor progression by miR-421/TUBB2A axis in GC cells. (A–C) Proliferation analysis was performed by MTT and colony formation assays in AGS and HGC-27 cells transfected with circ_C16orf62+ miR-NC, circ_C16orf62+ miR-421, circ_C16orf62+ si-NC and circ_C16orf62+si-TUBB2A. (D, E) The analysis of migration and invasion was carried out by using transwell assay in transfected AGS and HGC-27 cells. * $P<0.05$.

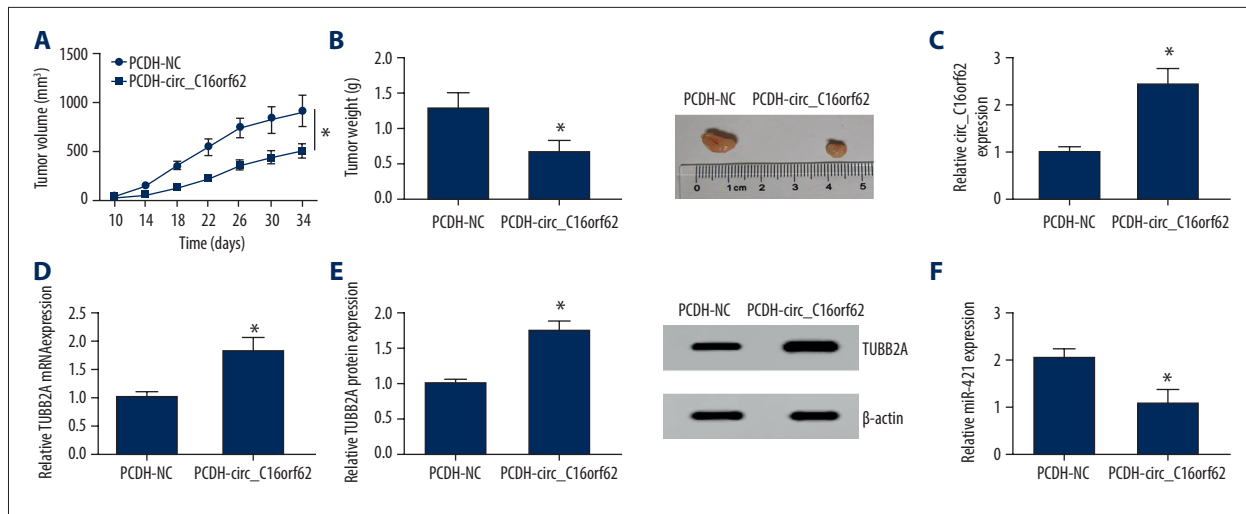


Figure 9. Circ_C16orf62 inhibited GC cell growth *in vivo*. (A, B) Tumor volume and tumor weight were measured in xenografts. (C, F) The levels of circ_C16orf62 and miR-421 in xenografts were detected by RT-qPCR. (D, E) Expression levels of TUBB2A were measured by RT-qPCR and western blot assays in xenografts. * $P < 0.05$.

To date, it has been widely believed that circRNAs could function as a ceRNA of miRNA to affect mRNA expression [27–29]. Moreover, post-transcriptional regulation of circ_C16orf62 was verified in GC cells by cytoplasmic expression of circ_C16orf62 in GC cells. In this manuscript, we have demonstrated that TUBB2A was expressed in GC tissues and cells, and TUBB2A silencing expedited GC cell proliferation, migration, and invasion, in accordance with a previous report [20]. Intriguingly, there was a positive correlation between circ_C16orf62 and TUBB2A in GC tissues. Hence, we explored whether circ_C16orf62 could regulate TUBB2A expression by interacting with some miRNAs. In this study, results of bioinformatic analysis and dual-luciferase reporter assay validated the binding relationship between miR-421 and circ_C16orf62 or TUBB2A in GC cells. MiR-421 was demonstrated to be upregulated in GC cells, in agreement with some previous studies [17,30,31]. Thus, miR-421 was chosen for more in-depth exploration in GC. In the research, our data confirmed the circ_C16orf62/miR-421/TUBB2A axis in GC cells. The rescue assays demonstrated that miR-421

or si-TUBB2A reversed the tumor-suppressive effect of circ_C16orf62 on GC growth, supporting a role for circ_C16orf62 in curbing tumor growth by regulating the miR-421/TUBB2A pathway in GC *in vitro*. In addition, an *in vivo* assay further verified that circ_C16orf62 inhibited GC tumor growth through the miR-421/TUBB2A axis.

Conclusions

To sum up, our results demonstrate that circ_C16orf62 suppresses GC tumor growth partly via the miR-421/TUBB2A axis *in vitro* and *in vivo*. This study suggests that circ_C16orf62 could be a therapeutic target in GC treatment.

Ethics statement

The current study was approved by the ethical review committee of Yantai Yuhuangding Hospital.

References:

- Bray F, Ferlay J, Soerjomataram I et al: Global cancer statistics 2018: GLOBOCAN estimates of incidence and mortality worldwide for 36 cancers in 185 countries. *Cancer J Clin*, 2018; 68(6): 394–424
- Siegel RL, Miller KD: Cancer statistics, 2019. *CA Cancer Clin Oncol*, 2019; 69(1): 7–34
- Coburn N, Cosby R, Klein L et al: Staging and surgical approaches in gastric cancer: A systematic review. *Cancer Treat Rev*, 2018; 63: 104–15
- Guo JU, Agarwal V, Guo H et al: Expanded identification and characterization of mammalian circular RNAs. *Genome Biol*, 2014; 15(7): 409
- Meng X, Li X, Zhang P et al: Circular RNA: An emerging key player in RNA world. *Brief Bioinform*, 2017; 18(4): 547–57
- Li X, Yang L, Chen LL: The biogenesis, functions, and challenges of circular RNAs. *Mol Cell*, 2018; 71(3): 428–42
- Tang YY, Zhao P, Zou TN et al: Circular RNA hsa_circ_0001982 promotes breast cancer cell carcinogenesis through decreasing miR-143. *DNA Cell Biol*, 2017; 36(11): 901–8
- Zhang J, Liu H, Hou L et al: Circular RNA_LARP4 inhibits cell proliferation and invasion of gastric cancer by sponging miR-424-5p and regulating LATS1 expression. *Mol Cancer*, 2017; 16(1): 151
- Zhang XL, Xu LL, Wang F: Hsa_circ_0020397 regulates colorectal cancer cell viability, apoptosis and invasion by promoting the expression of the miR-138 targets TERT and PD-L1. *Cell Biol Int*, 2017; 41(9): 1056–64
- Li P, Yang X, Yuan W et al: CircRNA-Cdr1as exerts anti-oncogenic functions in bladder cancer by sponging microRNA-135a. *Cell Physiol Biochem*, 2018; 46(4): 1606–16

11. Han J, Zhao G, Ma X et al: CircRNA circ-BANP-mediated miR-503/LARP1 signaling contributes to lung cancer progression. *Biochem Biophys Res Commun*, 2018; 503(4): 2429–35
12. Guan YJ, Ma JY, Song W: Identification of circRNA-miRNA-mRNA regulatory network in gastric cancer by analysis of microarray data. *Cancer Cell Int*, 2019; 19: 183
13. Guo H, Ingolia NT, Weissman JS et al: Mammalian microRNAs predominantly act to decrease target mRNA levels. *Nature*, 2010; 466(7308): 835–40
14. Bartel DP: MicroRNAs: Genomics, biogenesis, mechanism, and function. *Cell*, 2004; 116(2): 281–97
15. Li J, Dong G, Wang B et al: miR-543 promotes gastric cancer cell proliferation by targeting SIRT1. *Biochem Biophys Res Commun*, 2016; 469(1): 15–21
16. Sun F, Yu M, Yu J et al: miR-338-3p functions as a tumor suppressor in gastric cancer by targeting PTP1B. 2018; 9(5): 522
17. Wu J, Li G, Yao Y et al: MicroRNA-421 is a new potential diagnosis biomarker with higher sensitivity and specificity than carcinoembryonic antigen and cancer antigen 125 in gastric cancer. *Biomarkers*, 2015; 20(1): 58–63
18. Yang P, Zhang M, Liu X et al: MicroRNA-421 promotes the proliferation and metastasis of gastric cancer cells by targeting claudin-11. *Exp Ther Med*, 2017; 14(3): 2625–32
19. Leandro-Garcia LJ, Leskela S, Landa I et al: Tumoral and tissue-specific expression of the major human beta-tubulin isoforms. *Cytoskeleton (Hoboken)*, 2010; 67(4): 214–23
20. Cui F, Zan X, Li Y et al: Grifola frondosa glycoprotein GFG-3a arrests S phase, alters proteome, and induces apoptosis in human gastric cancer cells. *Nutr Cancer*, 2016; 68(2): 267–79
21. Livak KJ, Schmittgen TD: Analysis of relative gene expression data using real-time quantitative PCR and the 2^{-ΔΔC_T} method. *Methods*, 2001; 25(4): 402–8
22. Zhong Y, Du Y, Yang X et al: Circular RNAs function as ceRNAs to regulate and control human cancer progression. *Mol Cancer*, 2018; 17(1): 79
23. Patop IL, Kadener S: circRNAs in cancer. *Curr Opin Genet Dev*, 2018; 48: 121–27
24. Ma HB, Yao YN, Yu JJ et al: Extensive profiling of circular RNAs and the potential regulatory role of circRNA-000284 in cell proliferation and invasion of cervical cancer via sponging miR-506. *Am J Transl Res*, 2018; 10(2): 592–604
25. Cao W, Zhao Y, Wang L et al: Circ0001429 regulates progression of bladder cancer through binding miR-205-5p and promoting VEGFA expression. *Cancer Biomark*, 2019; 25(1): 101–13
26. Wang Z, Zhao Y, Wang Y et al: Circular RNA circHIAT1 inhibits cell growth in hepatocellular carcinoma by regulating miR-3171/P TEN axis. *Biomed Pharmacother*, 2019; 116: 108932
27. Bai N, Peng E, Qiu X et al: circFBLIM1 act as a ceRNA to promote hepatocellular cancer progression by sponging miR-346. *J Exp Clin Cancer Res*, 2018; 37(1): 172
28. Wang YG, Wang T, Ding M et al: hsa_circ_0091570 acts as a ceRNA to suppress hepatocellular cancer progression by sponging has-miR-1307. *Cancer Lett*, 2019; 460: 128–38
29. Huang C, Deng H, Wang Y et al: Circular RNA circABCC4 as the ceRNA of miR-1182 facilitates prostate cancer progression by promoting FOX P4 expression. 2019; 23(9): 6112–19
30. Liu H, Gao Y, Song D et al: Correlation between microRNA-421 expression level and prognosis of gastric cancer. *Int J Clin Exp Pathol*, 2015; 8(11): 15128–32
31. Zhang W, Shi S, Jiang J et al: LncRNA MEG3 inhibits cell epithelial-mesenchymal transition by sponging miR-421 targeting E-cadherin in breast cancer. *Biomed Pharmacother*, 2017; 91: 312–19